

## Article

# Synthesis of Boron Carbide Powder via Rapid Carbothermal Reduction Using Boric Acid and Carbonizing Binder

Bing Feng <sup>\*</sup>, Hans-Peter Martin  and Alexander Michaelis

Fraunhofer Institute for Ceramic Technologies and Systems, Winterbergstrasse 28, 01277 Dresden, Germany

<sup>\*</sup> Correspondence: bing.feng@ikts.fraunhofer.de; Tel.: +49-351-2553-7991

**Abstract:** Raw material is one of the most decisive factors for the quality of sintered boron carbide ( $B_4C$ ) products, in the past, there were relatively successful efforts for the synthesis of  $B_4C$  powders via carbothermal reduction approaches. To prepare high-quality powder, a deeper understanding of the relationship between technological manufacturing parameters and resulting powder properties is required. In this paper, pure  $B_4C$  powders were synthesized by rapid carbothermal reduction (RCR) under  $B_2O_3$  excess conditions using boric acid and a carbonizing binder as  $B_2O_3$  and carbon source, respectively. The molar ratio of  $B_2O_3/C$  of starting mixtures was varied from 0.75:1 to 4:1. The effects of heat-treating temperature and starting composition on phase constitution, morphology as well as stoichiometry of the prepared powders were investigated. The studies show that the starting composition has no effect on the stoichiometry of the powders, all boron carbides synthesized at 1900 °C have a stoichiometric composition of  $B_4C$ . With increasing heating temperature and  $B_2O_3$  content in the starting composition, the particle size of  $B_4C$  was reduced. Uniform  $B_4C$  powders with an average grain size of 300 nm were synthesized at 1900 °C from a starting powder mixture with a molar ratio of  $B_2O_3/C = 4$ . A formation mechanism is proposed under large  $B_2O_3$  excess conditions. For the starting powder mixtures with a molar ratio of  $B_2O_3/C < 2$ , the formation of boron carbide occurs through both liquid–solid reaction and gas–solid reaction. Accordingly, the synthesized powders exhibit a morphology with mixed elongated platelets and small polyhedral particles. For the starting powder mixtures with a molar ratio of  $B_2O_3/C \geq 2$ , fine-sized  $B_4C$  particles were formed by a liquid–solid reaction.

**Keywords:** boron carbide; carbothermal reduction; powder synthesis; nano particles



**Citation:** Feng, B.; Martin, H.-P.; Michaelis, A. Synthesis of Boron Carbide Powder via Rapid Carbothermal Reduction Using Boric Acid and Carbonizing Binder. *Ceramics* **2022**, *5*, 837–847. <https://doi.org/10.3390/ceramics5040061>

Academic Editor:  
Mari-Ann Einarsrud

Received: 20 September 2022  
Accepted: 19 October 2022  
Published: 21 October 2022

**Publisher's Note:** MDPI stays neutral with regard to jurisdictional claims in published maps and institutional affiliations.



**Copyright:** © 2022 by the authors. Licensee MDPI, Basel, Switzerland. This article is an open access article distributed under the terms and conditions of the Creative Commons Attribution (CC BY) license (<https://creativecommons.org/licenses/by/4.0/>).

## 1. Introduction

Boron carbide is an advanced non-oxide ceramic. It possesses a set of outstanding properties such as a high melting point, high thermal stability, low density, high mechanical strength, extreme hardness and a high neutron absorption cross section [1–3]. These excellent properties make boron carbide a promising material for various industrial applications, including refractory devices, ballistic protection, wear resistance enhancement, material polishing, composite reinforcement and reactor control in nuclear technology [1–5]. In addition, boron carbide is a promising candidate material for high-temperature sensors and thermoelectric energy conversion due to its large Seebeck coefficients and material stability [6,7]. The outstanding properties of boron carbide are related to its unique crystal structure [1–3]. Boron carbide varies in a wide homogeneity range from 8.8 at% C ( $B_{10.4}C$ ) to 20 at% C ( $B_4C$ ) and has rhombohedral elementary cells composed of 12-atom icosahedra and 3-atom chains [1–3].

The properties of bulk sintered compacts are strongly influenced by the characteristics of the used raw materials. Therefore, preparation approaches for high-quality boron carbide have attracted great attention. Boron carbide can be synthesized by a variety of methods, such as vapor phase reaction of boron halides and hydrocarbon gases [8,9], carbothermal reduction of boron–oxygen compounds [10–16], magnesiothermic reduction

of boron trioxide [17], self-propagating high-temperature synthesis (SHS) [18,19] and direct reaction of elemental boron and carbon [20,21]. Among these methods, carbothermal reduction has been widely used for the preparation of boron carbide owing to its cost-effective starting materials and simple synthesis process. The general reaction of boron carbide formation by carbothermal reduction can be described as:



Based on this reaction, great efforts have been devoted to the synthesis of boron carbide using different boron and carbon sources. Sinha et al. [10] reported on the synthesis of  $\text{B}_4\text{C}$  from boric acid and citric acid gel precursor, Alizadeh et al. [11] formed  $\text{B}_4\text{C}$  particles by reacting  $\text{B}_2\text{O}_3$  with petroleum and carbon active, and Yanase et al. [12] prepared boron carbide powder from polyvinyl borate obtained by condensation of polyvinyl alcohol and boric acid. Nevertheless, free carbon residue and inhomogeneous particle size distribution of final powders are the common issues in these studies. For many industrial applications, high purity boron carbide powders with a fine particle size in the nanometer range are always desirable. For example, Moshtaghionun et al. [22] investigated the grain size dependence of hardness in sintered boron carbide ceramics. They showed that the hardness increased from 31 MPa to 40 MPa if the average  $\text{B}_4\text{C}$  grain size was reduced from 17  $\mu\text{m}$  to 120 nm. Hence, formation and morphology control of  $\text{B}_4\text{C}$  particles during the synthesis process are critical for property modification of sintered  $\text{B}_4\text{C}$  products with the desired grain size.

Weimer et al. [13,14] developed a graphite vertical tubular reactor and first reported a process for producing submicron  $\text{B}_4\text{C}$  particles using rapid carbothermal reduction (RCR) from an intimate mixture of  $\text{B}_2\text{O}_3$  and cornstarch. It was found that the intrinsic kinetics of Equation (1) were inherently fast and heat transfer limitations played a dominant role in the overall reaction process. Rapid heating could improve heat conduction of the reduction and resulted in a small crystallite size of boron carbide. Several research works have also reported on the synthesis of ultrafine boron carbide powders using the same method [23–25]. Miller et al. [23] produced  $\text{B}_4\text{C}$  particles with a size ranging from 205 to 350 nm by the rapid carbothermal reaction of boric acid and carbon black. Toksoy et al. [24] obtained submicron  $\text{B}_4\text{C}$  powder (450 nm) using boric acid and Vulcan carbon black with a large surface area ( $\sim 235 \text{ m}^2/\text{g}$ ) through rapid carbothermal reduction. The RCR powders showed improved sinterability compared with commercial  $\text{B}_4\text{C}$  powders; consequently, the mechanical properties of the sintered  $\text{B}_4\text{C}$  ceramics could be improved significantly [23–25]. Furthermore, it is possible to use the RCR  $\text{B}_4\text{C}$  powders as starting materials for coating, spraying and producing functional composite ceramics.

Generally, preparation of  $\text{B}_4\text{C}$  by the carbothermal route by Equation (1) is associated with loss of boron in the form of boron trioxide and/or boron suboxide [10]. Therefore, an excessive amount of  $\text{B}_2\text{O}_3$  in the starting composition (molar ratio  $\text{B}_2\text{O}_3/\text{C} > 2:7$ ) is needed to compensate for the boron loss [23,26]. In addition, the morphology control of boron carbide particles in the rapid carbothermal reduction under  $\text{B}_2\text{O}_3$ -rich conditions is strongly dependent on the used boron and carbon sources.

In the present work, boron carbide powders were synthesized by rapid heating of  $\text{B}_2\text{O}_3$  excess (carbon deficient) powder mixtures of boric acid and carbonizing binder. The effects of heat treatment temperature and starting composition on phase constitution, morphology as well as stoichiometry of prepared powders were studied.

## 2. Materials and Methods

Commercial boric acid powder (99.99% purity, ABCR, Karlsruhe, Germany) and carbonizing binder OPTAPIX CS 76 (20.0 wt% carbon yield after pyrolysis, Zschimmer & Schwarz, Lahnstein, Germany) were used as starting materials for  $\text{B}_2\text{O}_3$  and carbon sources, respectively. The compositions and detailed processing conditions of the starting powders are given in Table 1. The molar ratio of  $\text{B}_2\text{O}_3$  to carbon (both pyrolysis products) was varied between 0.75:1 and 4:1. In the first step, different aqueous solutions were

prepared by adding boric acid and carbonizing binder to deionized water under vigorous stirring at 80 °C. Subsequently, the solution mixtures were dried at 90 °C in an oven for 48 h to remove the water. The dried mixtures were pyrolyzed at 400 °C with a heating rate of 1 K/min for 1 h under an argon atmosphere. Spongy black masses were formed after pyrolysis. The obtained precursors, composed of B<sub>2</sub>O<sub>3</sub> and carbon, were crushed and screened to powder with a maximum particle size of 315 μm.

**Table 1.** Composition of starting powder mixtures, processing conditions, phase constitution and lattice parameters of synthesized boron carbide powders.

Samples	H <sub>3</sub> BO <sub>3</sub> / Carbonizing Binder Weight Ratio	B <sub>2</sub> O <sub>3</sub> /C * Molar Ratio	Final Temperature (°C)	Dwell Time (min)	Phases after Heat Treatment	Hexagonal Lattice Parameters of Boron Carbide #	
						a (Å)	c (Å)
S1	1.54:1	0.75:1	1300	20	B <sub>2</sub> O <sub>3</sub> , amorphous C	-	-
S2	1.54:1	0.75:1	1400	20	B <sub>2</sub> O <sub>3</sub> , graphite	-	-
S3	1.54:1	0.75:1	1500	20	B <sub>2</sub> O <sub>3</sub> , graphite	-	-
S4	1.54:1	0.75:1	1600	20	B <sub>4</sub> C, B <sub>2</sub> O <sub>3</sub> , graphite	-	-
S5	1.54:1	0.75:1	1700	20	B <sub>4</sub> C, few graphite	-	-
S6	1.54:1	0.75:1	1800	20	B <sub>4</sub> C	5.6063 ± 0.0004	12.0877 ± 0.0013
S7	1.54:1	0.75:1	1900	20	B <sub>4</sub> C	5.6068 ± 0.0002	12.0898 ± 0.0008
S8	2.06:1	1:1	1900	20	B <sub>4</sub> C	5.5985 ± 0.0002	12.0819 ± 0.0007
S9	3.09:1	1.5:1	1900	20	B <sub>4</sub> C	5.6016 ± 0.0002	12.0823 ± 0.0006
S10	4.12:1	2:1	1900	20	B <sub>4</sub> C	5.5978 ± 0.0002	12.0693 ± 0.0006
S11	5.15:1	2.5:1	1900	20	B <sub>4</sub> C	5.6019 ± 0.0014	12.0825 ± 0.0030
S12	6.19:1	3:1	1900	20	B <sub>4</sub> C	5.6024 ± 0.0002	12.0841 ± 0.0005
S13	7.21:1	3.5:1	1900	20	B <sub>4</sub> C	5.6015 ± 0.0002	12.0796 ± 0.0006
S14	8.25:1	4:1	1900	20	B <sub>4</sub> C	5.6016 ± 0.0002	12.0783 ± 0.0006

\* calculated B<sub>2</sub>O<sub>3</sub>/C molar ratio of the starting powders, the carbon yield of the carbonizing binder after pyrolysis is 20.0 wt%. It is assumed that there is no B<sub>2</sub>O<sub>3</sub> and C loss during pyrolysis. # obtained by Rietveld analysis.

The powder mixtures were filled into a specially designed high-density graphite cylinder of 30 mm inner diameter and 110 mm length, equipped with lids on both sides (Figure 1a). Two holes of 1 mm in diameter were drilled at the top of the graphite cylinder for degassing during reaction. The synthesis of boron carbide was performed in a high temperature furnace (Thermal Technology LLC, Santa Rosa, CA, USA, model No. 1000-45180-FP60) under flowing argon by a rapid heating up procedure (heating rate > 500 K/s, Figure 1b). The graphite cylinder with loaded precursor powders was first placed in a cold sample chamber of the furnace and then quickly lifted into the heating chamber, after the furnace was heated to the processing temperature of between 1300 °C and 1900 °C. The pressure inside the furnace was kept at 1 atm and the argon flow rate was 0.2 L/min. After a dwell time of 20 min at processing temperature, the graphite reactor was pulled from the heating chamber in the sample chamber and naturally cooled down to room temperature.

To study decomposition and phase reaction of the precursor mixtures during heat treatment, differential thermal analysis (DTA), thermogravimetry (TG) and derivative thermogravimetry (DTG) were carried out on an unpyrolyzed powder mixture with a molar ratio of B<sub>2</sub>O<sub>3</sub>/C = 2:1 using a Netzsch STA 449 F1 thermal analyzer at a temperature up to 1600 °C in argon. The heating rate of this experiment was 10 K/min. The phase composition of the synthesized boron carbide powders in Table 1 was determined by X-ray diffraction (XRD, Bruker D8) with Cu Kα (λ = 1.54178 Å) radiation, and the morphology was observed using field-emission scanning electron microscopy (FESEM, ULTRA 55; CARL ZEISS, Jena, Germany) equipped with an energy-dispersive X-ray (EDX) detector.

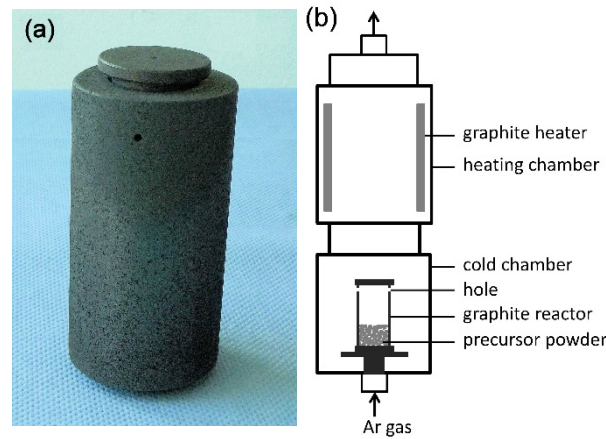


**Figure 1.** (a) Graphite cylinder reactor and (b) schematic illustration of a chamber furnace system for the synthesis of boron carbide powders.

### 3. Results and Discussion

#### 3.1. Thermal Analysis

The thermal analysis results of the unpyrolyzed powder mixture with a molar ratio of  $B_2O_3/C = 2:1$  (sample S10) are shown in Figure 2. It shows that there are two stages of mass loss. In the range of 60–380 °C, the TG curve exhibited a sharp mass loss of about 45%, corresponding to a broad endothermic peak in the DTA curve, which could be ascribed to the thermal dehydration of boric acid and carbonizing binder. According to Pankajavalli et al. [27],  $H_3BO_3$  decomposes through consecutive reactions, it firstly converts to metaboric acid  $HBO_2$  between 100 °C and 130 °C, and further converts to boron trioxide above 160 °C.

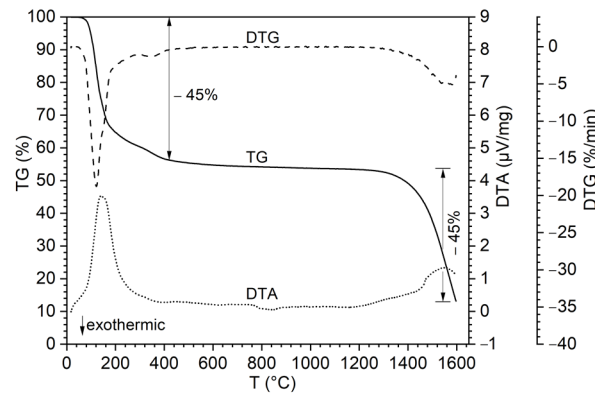
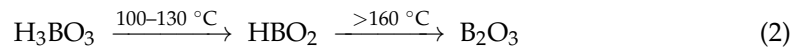


**Figure 2.** TG, DTG and DTA curves of a powder mixture with molar ratio  $B_2O_3/C = 2:1$ .

The overall reaction of the decomposition can be expressed as:



In the temperature interval between 380 °C and 1300 °C, no thermal effects and no notable weight loss were observed. Therefore, we chose 400 °C as the pyrolysis temperature for the starting powders to obtain a fully converted mixture of  $B_2O_3$  and carbon. The second stage of the mass loss started at around 1320 °C. The weight loss of this stage reached about 45% at 1600 °C, such a drastic mass loss is due to large amounts of gas generation during the carbothermal reduction. The evaporation of boron trioxide and boron suboxides formed in the heating process at high temperatures could be an additional contributor to the total mass loss [14,28].

### 3.2. Effect of Heat Treatment on Synthesis of Boron Carbide Powder

Figure 3 shows the XRD patterns of the starting powder mixture with a molar ratio of  $B_2O_3/C = 0.75:1$  and products (samples S1–S7) obtained by heat treatment at different temperatures of 1300–1900 °C for 20 min. As can be seen from Figure 3, the starting powders consist of only  $B_2O_3$  and amorphous carbon. After heat treating at 1300 °C, 1400 °C and 1500 °C, broad carbon peaks were found, indicating that nano-crystalline carbon was formed. The intensity of the  $B_2O_3$  peaks decreased gradually, indicating  $B_2O_3$  loss during heat treatment. After heat treatment at 1600 °C for 20 min, peaks of boron carbide were detected; however, there were still unreacted reactants in the product. By increasing the heat-treating temperature up to 1700 °C, the peaks corresponding to  $B_2O_3$  and carbon decrease. For the powder products obtained at 1800 °C and 1900 °C for 20 min, only peaks assigned to  $B_4C$  were observed.

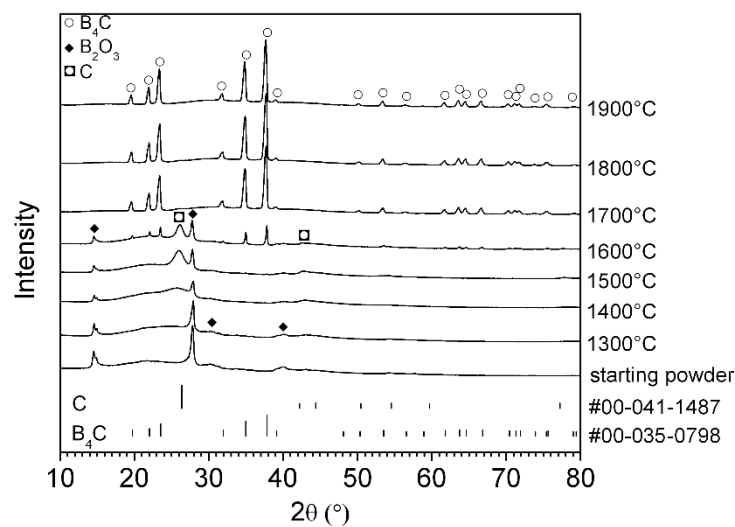


**Figure 3.** XRD patterns of starting powder and products prepared at 1300–1900 °C for 20 min from mixture with a molar ratio of  $B_2O_3/C = 0.75:1$ , powder diffraction file number: 00-041-1487 (graphite) and 00-035-0798 ( $B_4C$ ).

### 3.3. Effects of Heat Temperature on Morphology of Synthesized Boron Carbide Powder

SEM micrographs of the boron carbide powders (samples S5–S7) synthesized from a molar ratio of  $B_2O_3/C$  of 0.75:1 at 1700 °C, 1800 °C and 1900 °C for 20 min are illustrated in Figure 4a–d, respectively. The powders are characterized by the coexistence of fine particles and elongated platelets. When the heating temperature increased from 1700 °C to 1900 °C, more small polyhedral products with a particle size of 1–3  $\mu m$  were formed. The reduction in particle size is probably attributed to the increasing reaction temperature and heating rate, which will be discussed further below. The carbothermal reduction for the formation of  $B_4C$  is considered an interface-controlled process containing nucleation and growth of nuclei [28]. The nucleation rate in the early reaction stage can be written as [28,29]:

$$I = I_0 N_s \exp\left(-\frac{\Delta G}{kT}\right) \quad (4)$$

where  $I_0$  is the frequency of adding one more atom to a nucleus,  $N_s$  is the available nucleation site density and  $\Delta G$  is the nucleation barrier. Based on the classical nucleation theory, Foroughi et al. [28] studied the change of the nucleation barrier  $\Delta G$  for the  $B_4C$  nucleation in dependence on reaction temperature. It is found that the driving force for the carbothermal reduction becomes larger and the nucleation barrier  $\Delta G$  becomes smaller by increasing the process temperature. Accordingly, the nucleation rate from Equation (4) increases with increasing carbothermal reduction temperature. On the other hand, an increasing temperature gradient between the heating chamber and the cold

chamber (Figure 1b) was created by increasing the temperature from 1700 °C to 1900 °C, which increased the heating rate for the reaction. At higher heating rates and higher reaction temperatures, enhanced heat transfer and increased nucleation occur, leading to the formation of many small crystallites [14].

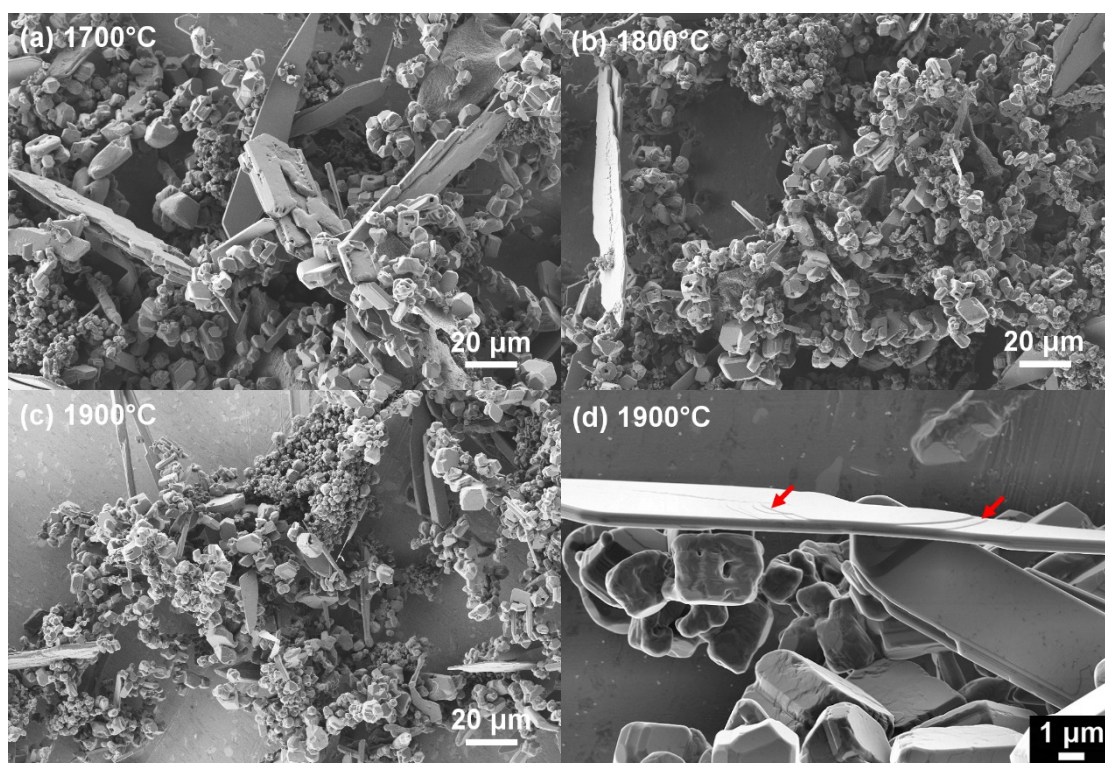


**Figure 4.** SEM micrographs of powders synthesized at different temperatures for 20 min from a mixture with a molar ratio of  $B_2O_3/C = 0.75:1$ , (a) 1700 °C, (b) 1800 °C, (c) and (d) 1900 °C, the arrows in (d) indicate the layered structure of synthesized boron carbide.

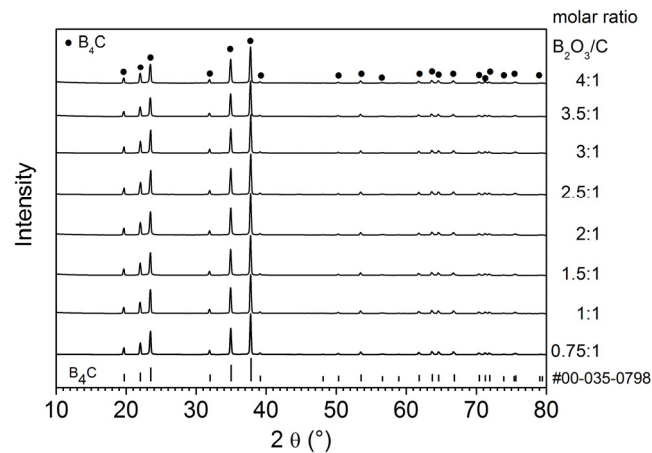
During the heating process, liquid  $B_2O_3$  is first formed ( $T_{\text{melting}} = 450$  °C) and partially evaporated in the form of  $B_2O_3$ / boron suboxides at high temperatures, as indicated by the thermal analysis and XRD analysis. The carbothermal reaction could occur through both the liquid and gaseous boron oxide with solid carbon. As a result, a morphology with mixed elongated platelets and small particles, like our work in Figure 4, is commonly reported in the  $B_4C$  products [16,28]. Jung et al. [26] attributed the formation of the elongated platelets with layered structure and smooth surfaces to a gas–solid interface reaction and the formation of fine-sized particles with truncated polyhedron morphology to a liquid–solid interface reaction.

### 3.4. Effect of Starting Composition on Stoichiometry of Synthesized Boron Carbide Powder

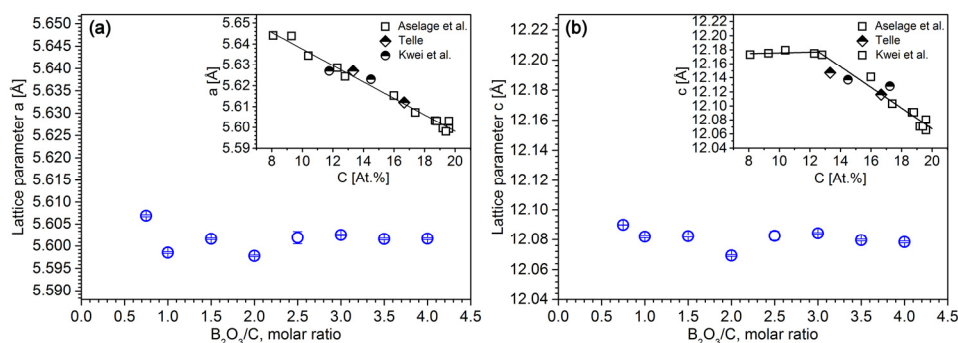
Theoretically, the molar ratio of  $B_2O_3/C$  for the synthesis of stoichiometric  $B_4C$  according to reaction (1) is about 0.286 (2:7). Due to the boron loss during the heating process, the application of excess  $B_2O_3$  is a common approach to obtain carbon-free products. Furthermore, the results of the study by Weimer et al. [13] suggest that a large excess of  $B_2O_3$  can yield boron-enriched boron carbide. To investigate the effects of starting composition on the stoichiometry of synthesized powders, the molar ratio of  $B_2O_3/C$  of the starting mixtures was varied from 0.75:1 to 4:1.

Figure 5 presents the XRD patterns of the prepared products (samples S7–S14), obtained at 1900 °C for 20 min. It reveals that the carbothermal reduction was completed for all powders and only peaks of the boron carbide phase were detected. Based on the XRD data, the hexagonal lattice parameters of the powders were determined using Rietveld

refinement and are listed in Table 1. It is well known that the lattice parameters of boron carbides are correlated with the carbon content of the B-C lattice (Figure 6 insets). The lattice parameter  $a$  experiences a steady increase toward more boron-rich stoichiometries, whereas a change in the slope at about 13 at% C is observed for the compositional dependence of the lattice parameter  $c$  [3]. Comparison of the lattice parameters in our study shows that large excess  $B_2O_3$  has hardly any influence on the stoichiometry of the resulting boron carbides (Figure 6). All prepared powders can be assigned to a stoichiometric boron carbide phase  $B_4C$ . The values of the lattice parameters are comparable with those of the standard  $B_4C$  (PDF 00-035-0798,  $a = 5.6003 \text{ \AA}$  and  $c = 12.086 \text{ \AA}$ ). Weimer et al. [13] studied the effect of processing temperature and initial boron to carbon molar ratio on product composition for the  $B_2O_3$ -C system using thermodynamic equilibrium calculations. The results showed that  $B_4C$  is the stable reaction product for a stoichiometric feed composition (molar ratio  $B_2O_3/C = 0.276$ ) up to its melting point (2743 K). In the presence of excess  $B_2O_3$ , boron-enriched boron carbides can be synthesized at temperatures above 2300 K. The formation of the stoichiometric  $B_4C$  phase in our study may be attributed to the lower heat-treating temperature.



**Figure 5.** XRD patterns of products synthesized at 1900 °C for 20 min using mixtures with a molar ratio of  $B_2O_3/C$  from 0.75–4:1.



**Figure 6.** Dependence of hexagonal lattice parameters  $a$  (a) and  $c$  (b) of boron carbides synthesized at 1900 °C for 20 min on the starting molar ratio of  $B_2O_3/C$ , the insets show the dependence of the lattice parameters on carbon content, data from Aselage et al. [30], Kwei et al. [31] and Telle [32].

### 3.5. Effect of Starting Composition on Morphology of Synthesized Boron Carbide Powder

Figure 7 shows SEM micrographs of boron carbide powders synthesized at 1900 °C for 20 min using a starting mixture with different  $B_2O_3/C$  molar ratios. It is seen that the amount of the elongated boron carbide platelets decreases with increasing  $B_2O_3/C$  ratios. For the powder products obtained from a  $B_2O_3/C$  ratio of 2 or greater, only fine-sized  $B_4C$  particles were formed. In addition, the particle sizes decreased from micron-

to submicron-sized range as the  $B_2O_3/C$  ratios increased from 2 to 4. The  $B_4C$  powders produced from a starting mixture with a molar ratio of  $B_2O_3/C = 4$  exhibit a narrow particle size distribution and the average particle size is approximately 300 nm. The change of the morphology in Figure 7 indicates that the formation of  $B_4C$  for mixtures with a molar ratio of  $B_2O_3/C \geq 2$  may take place completely through the direct reaction of liquid boron oxide with carbon.

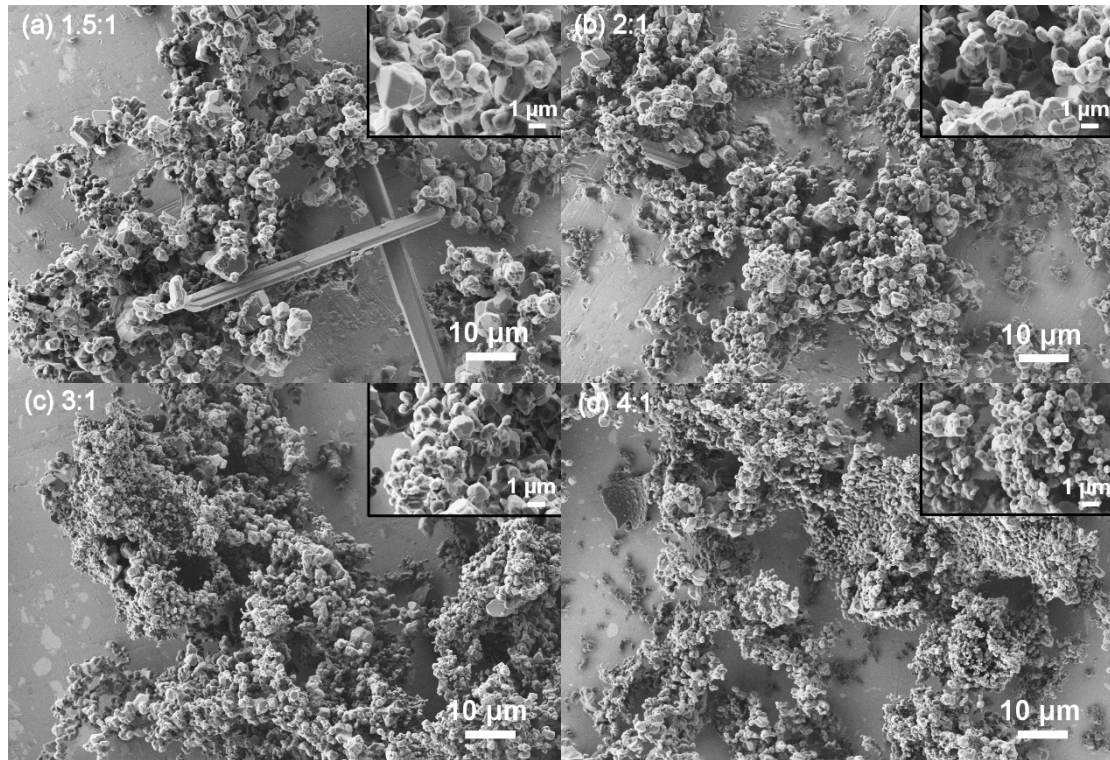
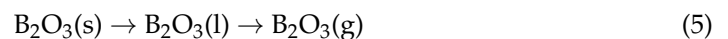


**Figure 7.** SEM micrographs of  $B_4C$  powders synthesized at  $1900\text{ }^\circ\text{C}$  for 20 min from starting mixtures with different  $B_2O_3/C$  molar ratios, (a) 1.5:1, (b) 2:1, (c) 3:1 and (d) 4:1.

### 3.6. Formation Mechanism

Based on the study of process kinetics, Weimer et al. [14] reported that the formation of boron carbide by carbothermal reduction is highly dependent on the phase changes of reactant boron oxide (solid  $B_2O_3 \rightarrow$  liquid  $B_2O_3 \rightarrow$  gaseous  $B_2O_3$ /boron suboxides), the heating rate and the ultimate temperature. The formation process of boron carbide may include the following reactions:



The gaseous boron suboxide ( $B_2O_2$ ) is generated at about  $1277\text{ }^\circ\text{C}$  according to Equation (6), and the formation is more favorable at high temperatures [33]. Weimer et al. [14] observed a change in the mechanism from liquid–solid reaction (Equation (7)) to gas–solid reaction (Equation (9)) at about  $1700\text{ }^\circ\text{C}$ . However, in the case of a large  $B_2O_3$  excess, the influence of starting composition on the reaction mechanism should be considered. Based on the results of our study, we propose the formation mechanism for boron carbide with respect to a large  $B_2O_3$ -rich environment, which is presented in Figure 8. For the starting

mixtures with a molar ratio of  $B_2O_3/C < 2$ , part of the carbon surface was covered by liquid  $B_2O_3$  during heat treatment. Both liquid–solid reaction and gas–solid reaction could occur simultaneously, resulting in fine-sized and elongated platelet  $B_4C$  powders, respectively. When the molar ratio of  $B_2O_3/C \geq 2$ , all the carbon particles were covered by  $B_2O_3$  liquid and there was no free carbon surface available for a gas–solid reaction. As a result, the formation of  $B_4C$  takes place only by liquid–solid reaction. The gaseous  $B_2O_3/B_2O_2$  has no contribution to the synthesis of boron carbide, the resulting  $B_4C$  powders are uniform and very fine.

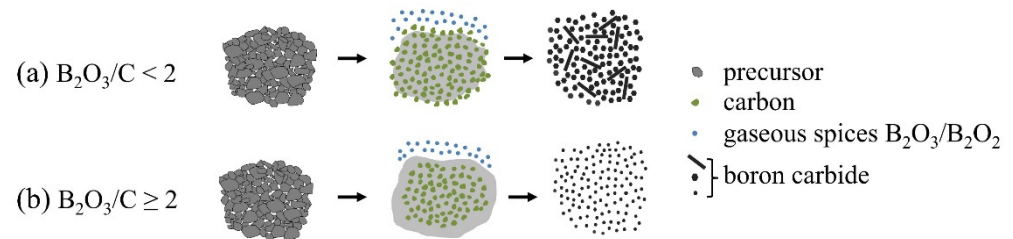


**Figure 8.** Schematic representation of formation mechanism of boron carbide particles for starting mixtures with different  $B_2O_3/C$  molar ratios, (a)  $B_2O_3/C < 2$  and (b)  $B_2O_3/C \geq 2$ .

#### 4. Conclusions

In this study, the synthesis of boron carbide powders using rapid carbothermal reduction from boric acid and carbonizing binder was investigated. Boron carbide powders without free carbon were successfully prepared from starting mixtures with a molar ratio of  $B_2O_3/C$  from 0.75:1 to 4:1. The starting composition has no effect on the stoichiometry of the products, all synthesized boron carbides have a stoichiometric composition of  $B_4C$ , which is attributed to the low processing temperatures. The particle size of the  $B_4C$  powders was strongly affected by the heat-treating temperatures and  $B_2O_3/C$  molar ratios. The nucleation rate of primary boron carbide was increased with increasing temperature and heating rate, resulting in the particle size reduction of  $B_4C$ .

In addition, it is found that for the starting mixtures with a molar ratio of  $B_2O_3/C < 2$  the formation of boron carbide occurs through both liquid–solid reaction and gas–solid reaction. Accordingly, the synthesized powders exhibit platelet-shaped and fine-sized morphology. For the starting mixtures with  $B_2O_3/C \geq 2$ , uniform and fine-sized  $B_4C$  particles were formed only by liquid–solid reaction. Our study demonstrates that the rapid carbothermal reduction approach provides a simple way to achieve high purity submicro  $B_4C$  powders. Further work should be done to identify the characteristics of the produced powders, such as purity, particle size distribution and bulk density. The sinterability and mechanical properties of sintered RCR powders should also be tested.

**Author Contributions:** B.F. contributed to the conceptualization, methodology, investigations, validation, visualization, and writing—original draft; H.-P.M. contributed to the conceptualization, funding acquisition, and writing—review and editing; A.M. supervised the research. All authors have read and agreed to the published version of the manuscript.

**Funding:** This research was funded by the 7th Framework Program of the European Commission, grant number EU FP/263306.

**Institutional Review Board Statement:** Not applicable.

**Informed Consent Statement:** Not applicable.

**Data Availability Statement:** Not applicable.

**Acknowledgments:** The authors would like to thank Maria Berger for the SEM micrographs and Sabine Henschke for the XRD analysis. We also thank Bernd Weise for the technical assistance in the heat-treating experiments.

**Conflicts of Interest:** The authors declare no conflict of interest. The funders had no role in the design of the study; in the collection, analyses, or interpretation of data; in the writing of the manuscript; or in the decision to publish the results.

## References

1. Thevenot, F. Boron carbide—A comprehensive review. *J. Eur. Ceram. Soc.* **1990**, *6*, 205–225. [[CrossRef](#)]
2. Suri, A.K.; Subramanian, C.; Sonber, J.K.; Murthy, T.C. Synthesis and consolidation of boron carbide: A review. *Int. Mater. Rev.* **2010**, *55*, 4–40. [[CrossRef](#)]
3. Domnich, V.; Reynaud, S.; Haber, R.A.; Chhowalla, M. Boron carbide: Structure, properties, and stability under stress. *J. Am. Ceram. Soc.* **2011**, *94*, 3605–3628. [[CrossRef](#)]
4. Walley, S.M. Historical review of high strain rate and shock properties of ceramics relevant to their application in armour. *Adv. Appl. Ceram.* **2010**, *109*, 446–466. [[CrossRef](#)]
5. Seiler, N.; Bertrand, F.; Marchand, O.; Repetto, G.; Ederli, S. Investigations on boron carbide oxidation for nuclear reactors safety—General modelling for ICARE/CATHARE code applications. *Nucl. Eng. Des.* **2008**, *238*, 820–836. [[CrossRef](#)]
6. Feng, B.; Martin, H.P.; Michaelis, A. In Situ Preparation and Thermoelectric Properties of  $B_4C_{1-x}-TiB_2$  Composites. *J. Electron. Mater.* **2013**, *42*, 2314–2319. [[CrossRef](#)]
7. Feng, B.; Martin, H.P.; Michaelis, A. Preparation and Characterization of  $B_4C-HfB_2$  Composites as Material for High-Temperature Thermocouples. *Crystals* **2022**, *12*, 621. [[CrossRef](#)]
8. Karaman, M.; Sezgi, N.A.; Dogu, T.; Ozbelge, H.O. Kinetic investigation of chemical vapour deposition of  $B_4C$  on Tungsten substrate. *AIChE J.* **2006**, *52*, 4161–4166. [[CrossRef](#)]
9. Santos, M.J.; Silvestre, A.J.; Conde, O. Laser-assisted deposition of r- $B_4C$  coatings using ethylene as carbon precursor. *Surf. Coat. Tech.* **2002**, *151*, 160–164. [[CrossRef](#)]
10. Sinha, A.; Mahata, T.; Sharma, B.P. Carbothermal route for preparation of boron carbide powder from boric acid-citic acid gel precursor. *J. Nucl. Mater.* **2002**, *301*, 165–169. [[CrossRef](#)]
11. Alizadeh, A.; Nassaj, E.T.; Ehsani, N.; Baharvandi, H.R. Production of boron carbide powder by carbothermic reduction from boron oxide and petroleum coke or carbon active. *Adv. Appl. Ceram.* **2006**, *105*, 291–296. [[CrossRef](#)]
12. Yanase, I.; Ogawara, R.; Kobayashi, H. Synthesis of boron carbide powder from polyvinyl borate precursor. *Mater. Lett.* **2009**, *63*, 91–93. [[CrossRef](#)]
13. Weimer, A.W.; Roach, R.P.; Haney, C.N.; Moore, W.G.; Rafaniello, W. Rapid carbothermal reduction of boron oxide in a graphite transport reactor. *AIChE J.* **1991**, *37*, 759–768. [[CrossRef](#)]
14. Weimer, A.W.; Moore, W.G.; Roach, R.P.; Hitt, J.E.; Dixit, R.S. Kinetics of carbothermal reduction synthesis of boron carbide. *J. Am. Ceram. Soc.* **1992**, *75*, 2509–2514. [[CrossRef](#)]
15. Tumanov, Y.N. The synthesis of boron carbide in a high frequency electromagnetic field. *J. Less Common Met.* **1979**, *67*, 521–529. [[CrossRef](#)]
16. Khanra, A.K. Production of boron carbide powder by carbothermal synthesis of gel material. *Bull. Mater. Sci.* **2007**, *30*, 93–96. [[CrossRef](#)]
17. Mohanty, R.M.; Balasubramanian, K.; Seshadri, S.K. Multiphase formation of boron carbide in  $B_2O_3-Mg-C$  based micropyretic process. *J. Alloys Compd.* **2007**, *441*, 85–93. [[CrossRef](#)]
18. Alkan, M.; Seref Sonmez, M.; Derin, B.; Yücel, O. Effect of initial composition on boron carbide production by SHS process followed by acid leaching. *Solid State Sci.* **2012**, *14*, 1688–1691. [[CrossRef](#)]
19. Aghili, S.; Panjepour, M.; Meratian, M.; Hadadzadeh, H. Effects of boron oxide composition, structure, and morphology on  $B_4C$  formation via the SHS process in the  $B_2O_3-Mg-C$  ternary system. *Ceram. Int.* **2020**, *46*, 7223–7234. [[CrossRef](#)]
20. Ramos, A.S.; Taguchi, S.P.; Ramos, E.C.T.; Arantes, V.L.; Ribeiro, S. High-energy ball milling of powder B-C mixtures. *Mater. Sci. Eng.* **2006**, *A422*, 184–188. [[CrossRef](#)]
21. Roszeitis, S.; Feng, B.; Martin, H.P.; Michaelis, A. Reactive sintering process and thermoelectric properties of boronrich boron carbides. *J. Eur. Ceram. Soc.* **2014**, *34*, 327–336. [[CrossRef](#)]
22. Moshtaghion, B.M.; Gomez-Garcia, D.; Dominguez-Rodriguez, A.; Todd, R.I. Grain size dependence of hardness and fracture toughness in pure near fully-dense boron carbide ceramics. *J. Eur. Ceram. Soc.* **2016**, *36*, 1829–1834. [[CrossRef](#)]
23. Miller, S.; Toksoy, F.; Rafaniello, W.; Haber, R. Submicron boron carbide synthesis through rapid carbothermal reduction. In *Advances in Ceramic Armor VIII*; John Wiley & Sons Inc.: Hoboken, NJ, USA, 2012; pp. 195–207.
24. Toksoy, M.F.; Rafaniello, W.; Xie, K.Y.; Ma, L.; Hemker, K.J.; Haber, R.A. Densification and characterization of rapid carbothermal synthesized boron carbide. *Int. J. Appl. Ceram. Technol.* **2017**, *14*, 443–453. [[CrossRef](#)]
25. Toksoy, M.F.; Haber, R.A. Modification of commercial boron carbide powder using Rapid Carbothermal Reduction. *Int. J. Appl. Ceram. Technol.* **2019**, *16*, 1120–1125. [[CrossRef](#)]
26. Jung, C.H.; Lee, M.J.; Kim, C.J. Preparation of carbon-free  $B_4C$  powder from  $B_2O_3$  oxide by carbothermal reduction process. *Mater. Lett.* **2004**, *58*, 609–614. [[CrossRef](#)]
27. Pankajavalli, R.; Anthonysamy, S.; Ananthasivan, K.; Vasudeva Rao, P.R. Vapour pressure and standard enthalpy of sublimation of  $H_3BO_3$ . *J. Nucl. Mater.* **2007**, *362*, 128–131. [[CrossRef](#)]

28. Foroughi, P.; Cheng, Z. Understanding the morphological variation in the formation of B<sub>4</sub>C via carbothermal reduction reaction. *Ceram. Int.* **2016**, *42*, 15189–15198. [[CrossRef](#)]
29. Xin, F.; Jun, J.; Chao, L.; Zhi-Yang, Y.; Lea, S.; Jun, Y. Re-entrant-groove-assisted VLS growth of boron carbide five-fold twinned nanowires. *Chin. Phys. Lett.* **2009**, *26*, 086110. [[CrossRef](#)]
30. Aselage, T.L.; Tissot, R.G. Lattice constants of boron carbides. *J. Am. Ceram. Soc.* **1992**, *75*, 2207–2212. [[CrossRef](#)]
31. Kwei, G.H.; Morosin, B. Structures of the boron-rich boron carbides from neutron powder diffraction: Implications for the nature of the inter-icosahedral chains. *J. Phys. Chem.* **1996**, *100*, 8031–8039. [[CrossRef](#)]
32. Telle, R. Structure and Sintering Behaviour of Multiphase Ceramics in the Hard Material System B<sub>4</sub>C-Si. Ph.D. Thesis, Stuttgart University, Stuttgart, Germany, 1985.
33. Rentzepis, P.; White, D.; Walsh, P.N. The reaction between B<sub>2</sub>O<sub>3</sub>(l) and C(s): Heat of formation of B<sub>2</sub>O<sub>2</sub>(g). *J. Phys. Chem.* **1960**, *64*, 1784–1787. [[CrossRef](#)]